

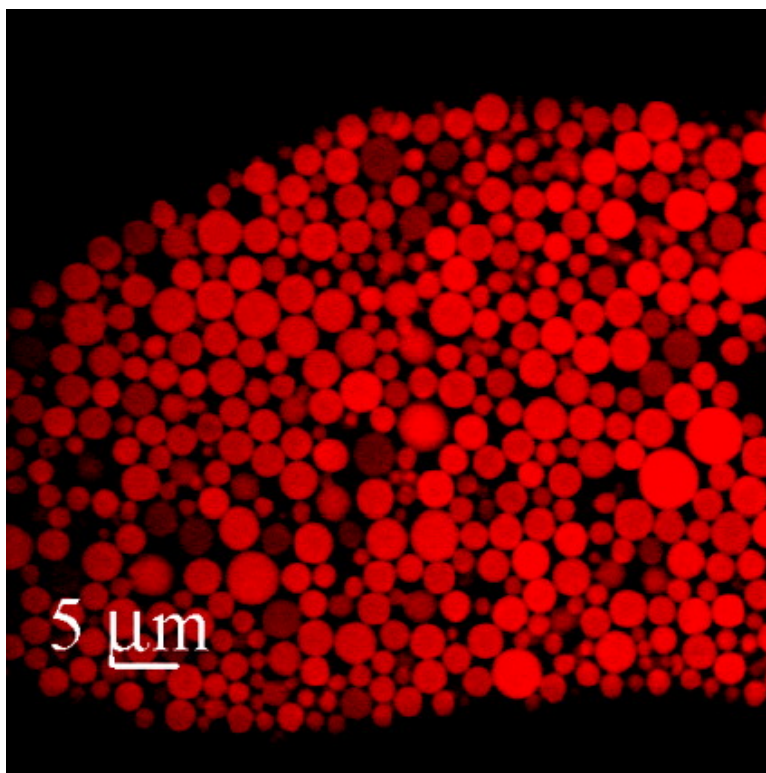
Article

Novel PVA-Based Hydrogel Microparticles for Doxorubicin Delivery

Francesca Cavalieri, Ester Chiessi, Raffaella Villa, Lucia
Vigano#, Nadia Zaffaroni, Mark F. Telling, and Gaio Paradossi

Biomacromolecules, **2008**, 9 (7), 1967-1973 • DOI: 10.1021/bm800225v • Publication Date (Web): 06 June 2008

Downloaded from <http://pubs.acs.org> on March 12, 2009



More About This Article

Additional resources and features associated with this article are available within the HTML version:

- Supporting Information
- Access to high resolution figures
- Links to articles and content related to this article
- Copyright permission to reproduce figures and/or text from this article



ACS Publications
High quality. High impact.

Biomacromolecules is published by the American Chemical Society, 1155
Sixteenth Street N.W., Washington, DC 20036

[View the Full Text HTML](#)



Novel PVA-Based Hydrogel Microparticles for Doxorubicin Delivery

Francesca Cavalieri,[†] Ester Chiessi,[†] Raffaella Villa,[‡] Lucia Viganò,[§] Nadia Zaffaroni,[‡] Mark F. Telling,^{||} and Gaio Paradossi^{*,†}

Dipartimento di Scienze e Tecnologie Chimiche, Università di Roma Tor Vergata, 000133 Roma, Italy, Dipartimento di Oncologia Sperimentale e Dipartimento di Oncologia Medica, Fondazione IRCCS Istituto Nazionale dei Tumori, 20133 Milano, Italy, and Rutherford Appleton Laboratory, Chilton Didcot OX11 0QX, United Kingdom

Received February 29, 2008; Revised Manuscript Received April 22, 2008

Micro- and nanoparticles are considered suitable drug delivery systems for their unique features, such as a large surface to volume ratio, and for the possibility to tune their size and hydrophobicity. A polymer/polymer/water emulsion method was used for producing a chemically cross-linked hydrogel made of poly(vinyl alcohol) and of poly(methacrylate) moieties. Mesoscopic investigation of the microparticles was accomplished by laser scanning confocal microscopy. Dynamics of confined water within the gel meshes was studied by quasi-elastic incoherent neutron scattering. Succinylation of these particles allowed an efficient loading with a maximum doxorubicin payload of about 50% (w/w) of dry microparticles. To evaluate the potentials of such a microdevice for drug delivery, LoVo colon cancer cells have been exposed to doxorubicin loaded microparticles to study the in vitro efficiency of the payload release and the consequent cytotoxic effect.

Introduction

The new perspectives offered by genomics and proteomics are challenging the science and technology of drug delivery in suggesting new methods for the sustained/controlled release of drug molecules or therapeutic systems in living systems.¹ Moreover, the increasing understanding at molecular and mesoscopic level of biointerface processes,² such as cellular bioadhesion,³ blood coagulation,⁴ and protein accumulation on particle surfaces,⁵ has opened new routes toward a multifunctional delivery device, with the aim to support the release of pharmacological relevant compounds in both diagnostics and therapeutic approaches. The natural crossing between the role played by the bioactive molecule and carrier functions is a result of this perspective in modern drug design, where the concept of “drug” also includes a device and where targeting, controlled release, bioavailability, and bioelimination are achieved by concerted processes between the cell, the therapeutically active molecule, and the cargo matrix.⁶

Micro- and nanoparticles are considered as promising injectable devices capable of providing many of the functions requested in a controlled delivery. However, a caveat is necessary, as little is known about viability of these cargo particles^{7,8} in terms of cytotoxicity and response of the primary immunosystem (phagocytosis).⁹

We have fabricated microparticles based on the cross-linking of emulsions of methacrylate derivatized poly(vinyl alcohol), PVA-MA, in the presence of dextran T70, exploiting the immiscibility of this polymer with PVA-MA. PVA-MA has been studied in our laboratory as potential material for in situ vitreous

replacement achieved by photopolymerization at 350 nm in the presence of a photoinitiator.¹⁰ This synthetic route can be suitably modified to tailor the hydrogel swelling by varying the cross-linking degree.

In this paper, we report on the obtainment of microparticles by a photoreticulation in a polymer/polymer/water emulsion as part of a study on the formulation of new multifunctional delivery systems. The macroscopic release properties of microparticles are dictated by the microscopic diffusion pattern of the water confined in the network meshes and by the polymer network segmental motions. Moreover, the use of such delivery devices for carrying high molecular weight molecules, as in the case of gene therapy, requires the retention of native conformation of the active agent. To clarify these aspects, we have investigated the dynamic processes occurring in the microparticle hydrogels of PVA-MA and the polymer–water interplay by means of quasi-elastic incoherent neutron scattering (QENS).¹¹ The availability of experimental approaches using high-flux neutron sources provides the possibility to study the dynamic properties of water at a molecular level. With modern time-of-flight spectrometers, polymer segmental dynamics can also be accessed by neutron scattering by replacing water with D₂O. The large difference between the incoherent scattering cross-section of hydrogen and deuterium allows enhancement of the QENS contribution of polymer network protons.

In the perspective to use our device for the delivery of anticancer drugs,¹² the loading/release properties of the microbead hydrogel were evaluated in vitro with the anticancer drug doxorubicin (DX) on succinoylated microparticles. This modification was made to increase the drug payload by favorable electrostatic interactions. In addition, the uptake of released DX by LoVo human colon carcinoma cells as well as the cytotoxic effect of DX loaded on microparticles were studied.

* To whom correspondence should be addressed. E-mail: paradossi@stc.uniroma2.it.

[†] Università di Roma Tor Vergata.

[‡] Dipartimento di Oncologia Sperimentale, Fondazione IRCCS Istituto Nazionale dei Tumori.

[§] Dipartimento di Oncologia Medica, Fondazione IRCCS Istituto Nazionale dei Tumori.

^{||} Rutherford Appleton Laboratory.

Experimental Section

Materials. Poly (vinyl alcohol), PVA, and succinic anhydride were Sigma products. PVA number and weight average molecular weights determined in this laboratory were 30000 ± 5000 and 70000 ± 10000 g/mol, respectively. Blue dextran was a Sigma product, with an average molecular weight of 200000 (supplier indication). Dextran T70, with a number average molecular weight of 70000 g/mol, was purchased from Amersham Pharmacia Biotech.

Dimethyl sulfoxide (DMSO), acetone, sodium metaperiodate, trichloro acetic acid (TCA), and inorganic acids and bases were RPE grade products from Carlo Erba. Fluorescein isothiocyanate isomer 1, FITC, was purchased from Fluka.

4-(*N,N*-Dimethylamino)pyridine (DMAP) and glycidylmethacrylate (GMA) were purchased from Fluka and used without further purification. Photoinitiator 2-hydroxy-1-[4-(hydroxyethoxy)phenyl]-2-methyl-1-propanone (Irgacure 2959, Ciba) was used without further purification. Phosphate buffered saline (0.01 M) solution with 0.138 M NaCl and 0.0027 M KCl M at pH 7.4 (PBS) was a Sigma product. Trypan blue was a Sigma product, used without further purification.

All reagent grade chemicals were used without further purification. Water was Milli-Q purity grade ($18.2 \text{ M}\Omega \cdot \text{cm}$) produced with a deionization apparatus (PureLab) from USF-Elga. For QENS experiments, 99.9% pure D_2O from Aldrich was used.

Methods. *Methacryloyl-Derivative of Poly(vinyl alcohol), PVA-MA.* Details of the synthesis of this compound have been already described in a previous paper,¹⁰ following the route described by van Dijk-Wolthuis et al.^{13,14} for the synthesis of methacryloyl-dextran derivatives. In short, 10 g of PVA was dissolved in DMSO at 80 °C. After cooling, 5 g of DMAP was added, purging with N_2 for 1 h. Finally, a known amount of GMA was added in the proper molar ratio, with polymer repeating units. The reaction was carried out for 48 h at room temperature in darkness under stirring and stopped by neutralizing the solution with an equal molar amount of HCl with respect to DMAP. DMSO was replaced with water by exhaustive dialysis. The sample was stored as a freeze-dried powder.

After methacryloyl grafting, the determination of the degree of substitution, DS, defined as the number of methacrylated residues per 100 total residues, was carried out by ^1H NMR analysis.¹⁰ For microparticles preparation, a sample with DS = 4.7%, hereafter labeled PVAMA5, was used throughout this study.

PVAMA5 Microparticles Preparation. PVAMA5 microparticles were prepared, adapting the procedure outlined by Franssen and Hennink,¹⁵ using an emulsion technique based on polymer–polymer immiscibility in aqueous solutions. In a typical experiment, an aqueous solution containing dextran T40 at a concentration of 16% (w/v), PVAMA5 at 2% (w/v), and the UV photoinitiator Irgacure 2959 at 0.3% (w/v) was vigorously stirred by an UltraTurrax at 8000 rpm. After emulsification, the PVAMA5 in the dispersed phase was cross-linked by photopolymerization using a 365 nm light source at an intensity of $7 \text{ mW}/\text{cm}^2$ for 5 min. The cross-linked microparticles were purified by repeated washing and centrifugation steps.

Negatively Charged PVAMA5 Microparticles Preparation. PVA-MA5 microparticles were chemically modified by *O*-succinylation to introduce different amounts of monosuccinate groups ranging from 2.8 to 4% (mol/mol) of the total residues. Succinic anhydride (0.1 g) and DMAP (0.5 g) were added to a suspension of 1 g of PVAMA5 microparticles in 25 mL of anhydrous DMSO with stirring and under nitrogen flux. The suspension was kept at 40 °C for 24 h under nitrogen atmosphere and then neutralized and dialyzed against Milli Q quality water. The determinations reported here were made on microparticles with an *O*-succinylation degree of 4 mol %, determined by potentiometric titration (see details below) hereafter labeled PVAMA5S4.

Characterization of Microparticles. Particle size distribution was evaluated by dynamic light scattering, DLS, using a BI-200SM goniometer (Brookhaven Instruments Co.) equipped with a laser source at 532 nm. The autocorrelation functions were analyzed with the CONTIN algorithm.

Particle size and shape were also investigated by confocal laser scanning microscopy, CLSM, labeling the microparticles with FITC by coupling the dye to PVA hydroxyl groups.¹⁶ Fluorescent dye at a concentration of $10 \mu\text{M}$ was added in the dispersion. After several washings to remove the excess dye, confocal images were collected with an inverted microscope, Nikon PCM 2000 (Nikon Instruments) based on a galvanometer point-scanning mechanism, a single pinhole optical path, and a multiexcitation module equipped with an Ar^+ (488, 514 nm) and a He–Ne (543.5 nm) laser. A $60\times/1.4$ oil immersion objective was used for the observations. Microparticles average diameter and standard deviation were determined over a set of 200 microparticle images. Results were validated with ImageJ software package.

ζ -Potential and charge density measurements were carried out with a ζ -potential particle analyzer (Brookhaven, New York). Particle dispersion (1.5 mL) at a concentration of 1 g/L was loaded in the measuring cell using 0.01 M KCl as supporting electrolyte. The results reported were the average of six repetitive measurements.

UV–vis absorption measurements were carried out with a double beam JASCO 7850 spectrophotometer equipped with quartz 1 cm optical length cuvettes (Hellma).

QENS Experiments on PVAMA5 Microparticles. QENS experiments on PVAMA5 microparticles were performed at ISIS high flux neutron facility (Rutherford Appleton Laboratory, Chilton, U.K.) using the IRIS time-of-flight inverted geometry spectrometer in the configuration having the 002 reflection of pyrolytic graphite for the near-back-scattering crystal analyzer. Data processing has been described in a previous paper.¹¹ Microparticle samples in the presence of water or D_2O were prepared by isopiestic method: dry microparticles were exposed to water or D_2O at controlled humidity in a closed environment at room temperature.

Solvent uptake was determined by weighing out the samples before and after adsorption of the solvent. A microparticles layer of 2 mm was placed in the measuring aluminum cell consisting of two bolted plates, sealed with an Indium wire. Temperatures, from 10 to 60 °C, step 10 °C, were monitored by putting a heater in a notch in one of the plates. A typical run was carried out for 5 h under vacuum in a temperature-controlled environment equipped with a closed cycle refrigerator unit. The instrument energy resolution, determined by using vanadium slabs in the measuring cell, was $15 \mu\text{eV}$ as full width at half-maximum. Fifty channels covering an energy transfer window, from -0.4 to 0.9 meV , and corresponding to a momentum transfer, $q = (4\pi/\lambda) \sin \theta/2$, ranging from 0.44 to 1.55 \AA^{-1} , have been explored. The channels were binned into 20 q equally spaced values. Corrections for multiple scattering were not applied as the sample thickness was always lower than 0.3 mm. Raw data were corrected for absorption and background using the standard software package GUIDE available on site.

PVAMA5S4 Drug Loading and Release. In a typical DX loading process, 10 mg of PVAMA5S4 dry microparticles were suspended in 3 mL of aqueous DX at a concentration of $3.6 \times 10^{-5} \text{ M}$. After that, a constant absorbance of the suspension was reached, and the microparticles were centrifuged at 1000 rpm for 1 min prior to release study and transferred in 3 mL of MilliQ water. DX release was monitored by measuring the time dependence of the absorbance at 485 nm ($\epsilon_{485} = 11500 \text{ M}^{-1} \cdot \text{cm}^{-1}$). Release behavior was analyzed in terms of cumulative release index, M/M_{inf} , expressed as the ratio of cumulative moles of released DX over the moles of released DX at infinite time.

Cell Line and DX-Mediated Cytotoxicity. The LoVo human colon adenocarcinoma cell line obtained from American type Culture Collection was used in this study. According to growth profiles preliminary defined for the cell model, appropriate numbers of cells in the logarithmic growth phase were plated in each well of a 24-well plate and allowed to attach to the plastic surface for 24 h.¹⁷ For the analysis of DX cytotoxicity, cells were incubated with free drug (final concentration $1.8 \mu\text{M}$) or $10 \mu\text{L}$ /well of PVAMA5S4 microparticles loaded with DX (with a cargo amount of 1.5 mg per gram) for 2–48 h, followed by a 72 h incubation in drug-free medium at 37 °C in a

5% CO₂ humidified atmosphere in air. At the end of incubation, cells were trypsinised and counted in a particle counter (Coulter Counter, Coulter Electronics, Luton, U.K.). The percentages of adherent viable cells were determined by the Trypan blue dye exclusion test. Each experimental sample was run in triplicate. The results were expressed as the total number of adherent cells in drug-treated samples compared to control untreated samples.

HPLC Method for Detection of DX Release and Cellular Uptake. DX was measured by an HPLC method with online extraction to increase sensitivity, as previously reported.¹⁸ To measure DX release from microparticles and cellular uptake of DX, experiments were performed by seeding 1×10^5 cells into 24-well plate/0.5 mL. After 24 h, cells were incubated with 10 μ L of DX-loaded microparticles with a cargo amount of 1.5 mg/g at a concentration of 60 mg/mL in 0.5 mL of cell culture medium. For DX release, at different time points, samples of medium were collected, centrifuged to remove microparticles, frozen, and stored at -80° until HPLC analysis. After the addition of daunorubicin as internal standard, volumes of 0.2 mL of medium were injected and loaded onto a 4×4 mm cartridge (Lichrospher-100 RP-18; Merck, Darmstadt, Germany) arranged in a LichroGraf OSP-2/Online Sample Preparation Unit (Merck) at room temperature. Before medium loading, the cartridge was wetted with 90% acetonitrile–10% water (vol/vol) and equilibrated with 9 mL of ammonium acetate buffer (0.01 M, pH 7.5; AAB 7.5) at 3 mL/min flow. The samples were loaded onto cartridge with AAB 7.5 at 0.5 mL/min flow. After washing at 2 mL/min with 4 mL of AAB 7.5 and with 4 mL of 0.01 M AAB 3.9, the cartridge was automatically moved on line with the chromatographic system. The analytical system consisted of an HP1050 quaternary pump (Agilent Technologies, Santa Clara, CA), connected to a Superspher 100 RP-18 column (12.5 cm \times 4 mm) equipped with a Lichrospher 100 RP-18 precolumn (Merck). The HPLC separation was performed by a linear gradient from 30% acetonitrile/70% AAB 3.9 (vol/vol) to 60% acetonitrile/40% TAA 3.9 (vol/vol) in 7 min at 1 mL/min. DX and internal standard were detected by an HP-1046A fluorimeter (Agilent Technologies) at an excitation wavelength of 227 nm and at an emission wavelength of 552 nm.

For DX uptake, cells were washed twice with cold PBS to remove all microparticles and trypsinized. Pellets of cells were suspended in 80 μ L PBS and 30 μ L 5% TCA. After a 10 min incubation at 4 $^\circ$ C, samples were centrifuged at 14000 rpm for 5 min, and the supernatants were buffered to 7.4 by addition of 1 M Tris buffer. Total volume samples were transferred into autosampler vials and analyzed as previously indicated. For each single analytical run, a standard curve of DX was prepared in medium using the product of the highest purity commercially available for analytical purposes. Standard curve concentrations ranged from 0.005 to 10 μ M, and the response was calculated as peak height ratio of DX to internal standard. Two independent experiments were carried out, and each experimental point was tested in duplicate.

Results and Discussion

Delivery platforms based on PVA have been developed mainly as monolithic devices. Implantation of such systems can cause an unfavorable immune response that jeopardizes drug release. However, external application of transdermal patches has the difficulty of overcoming the natural barrier of the dermis. Sustained release can be achieved with the aid of ultrasounds or electric impulses.

In principle, nano- and microparticles are a reasonable solution to bypass the aforementioned delivery problems, as they can be injected. However, other not less important problems arise when cargo particles are injected. First, the size is the feature of the particle deciding its destiny. Phagocytosis and the lumen of peripheral capillaries rule on the particle size and size distribution.

Microparticles were obtained by an emulsion of methacryloyl-substituted PVA, with a degree of substitution of 4.7%,

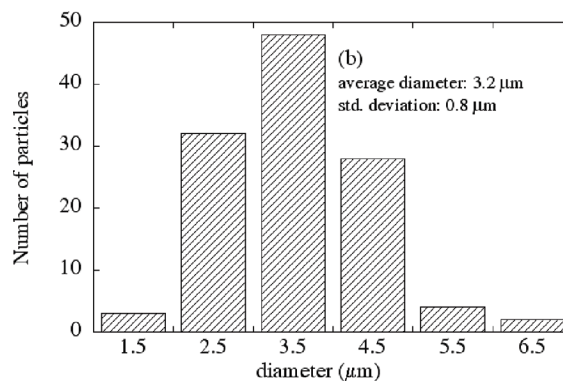
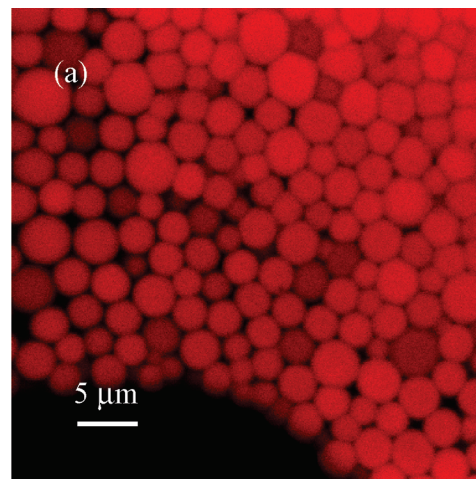


Figure 1. (a) CLSM image of PVAMA5 microparticles and (b) their size distribution.

PVAMA5, in an aqueous Dextran T70. Aqueous droplets of the vinyl moiety dispersed in the dextran-containing phase under vigorous stirring were UV irradiated in the presence of the photoinitiator to trigger a cross-linking process. An advantage of this method is the absence of any organic solvent during the whole process.

Confocal microscopy of the equatorial planes of the particles provided an evaluation of (Figure 1a,b) the average diameter of 3.2 μ m, with a standard deviation of 0.8 μ m.

The relatively narrow size distribution as well as the average diameter of the microparticles open the possibility of injecting this device for systemic administration, as the dimensions of the capillaries are comparable or slightly larger than the diameter of the largest microparticles fraction.

Microparticles porosity in terms of the average molecular weight between two cross-links was evaluated by the swelling method developed by Stenekes and Hennink,¹⁹ monitoring the increase in absorbance of the aqueous phase containing blue dextran due to particles swelling. The equilibrium volume fraction of the polymer microparticles is $\varphi_2 = 0.20$, with a reference polymer volume fraction $\varphi_0 = 0.80$, determined by the equilibrium composition after phase separation of the polymer/polymer emulsion. According to these findings, the number average molecular weight between cross-links of the PVAMA5 microparticles is 2400 ± 100 g/mol.

ζ -Potential measurements of PVAMA5 microparticles at a concentration of 1 mg/mL in the presence of 1 mM KCl as supporting electrolyte displayed a negative value of -14.47 mV. This finding was interpreted as indicative of the presence of residual charge at the particle interface, probably due to a partial hydrolysis of the methacryloyl moiety of the hydrogel.

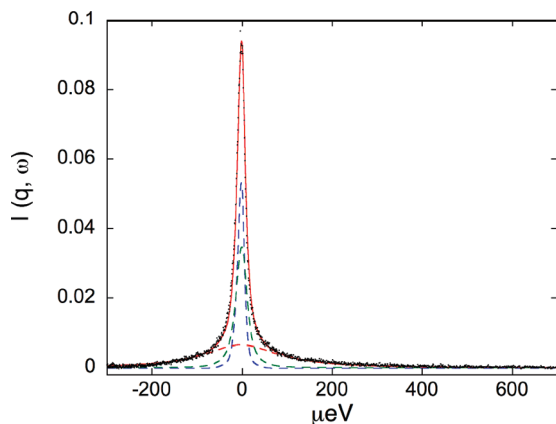


Figure 2. QENS spectrum of PVAMA5 microparticles in D₂O (dots) at 50 °C for $q = 0.69930 \text{ \AA}^{-1}$. Fitting eq 1 (continuous red line), $\text{EISF}\delta(\omega)$ (dashed blue line), $(1 - \text{EISF})[p_1L_1 + (1 - p_1)L_2]$ (dashed green and red lines, respectively).

The structure of PVAMA5 microparticles is intrinsically heterogeneous as the radical polymerization reaction involves only the side chain vinyl moiety. The resultant network is therefore made of PVA chains linked to polymethacrylate in analogy with the work of Stenekes and Hennicks¹⁹ and van Dijk-Wolthuis et al.²⁰ on the polymerization of hydroxyethyl methacryloyl derivative of dextran.

The microparticles have a more accessible-to-solvent external region made by the PVA chains and a hydrophobic internal core due to the presence of methacrylic strands. It can be expected that this structural heterogeneity is reflected on the dynamic behavior of water and on the segmental dynamics of the polymeric components. The diffusive processes occurring on this self-assembled system were studied by QENS.²¹ The broadening of the scattering law, $S(q, \omega)$, contains information about the dynamics of the matrix at molecular level.

The dynamic regimes present in a hydrogel particle can be attributed to differently relaxing parts of the network. Close to the grafting points, hydrophobic methacrylic chains and PVA chains have a reduced local mobility, whereas the polymer segments far from the network junctions will possess a faster dynamics. Therefore, the dynamic models used to extract the diffusion parameters of the polymeric moiety contain two relaxing contributions concerning the polymer.

We investigated the PVAMA5 system with an experimentally determined M_c of 2400 g/mol in three different solvation states: (i) saturated D₂O, (ii) a water content of 60% (g water/g swollen hydrogel), and (iii) saturated water, corresponding to a hydration degree of 93% (g water/g swollen hydrogel). In case (i), the $S(q, \omega)$ is described (see eq 1) by a normalized linear combination of two Lorentzians, L_1 , accounting for a slow diffusion process related to the nonexchangeable protons of PVA and polymethacrylate chains and/or deuterated water tightly bound to the polymer, and L_2 , for a faster diffusing process relative to more mobile protons of PVA chains and loosely coordinated heavy water:

$$S(q, \omega) = A\{\text{EISF}\delta(\omega) + (1 - \text{EISF})[p_1L_1 + (1 - p_1)L_2]\} + \text{bkg} \quad (1)$$

where A is a normalization factor, EISF is the elastic fraction of the total scattering intensity, and p_1 is the mole fraction of protons characterized by a slow translational displacement. Use of eq 1, convoluted with the experimental resolution, as fitting equation for the experimental $I(q, \omega)$, (Figure 2), allows the

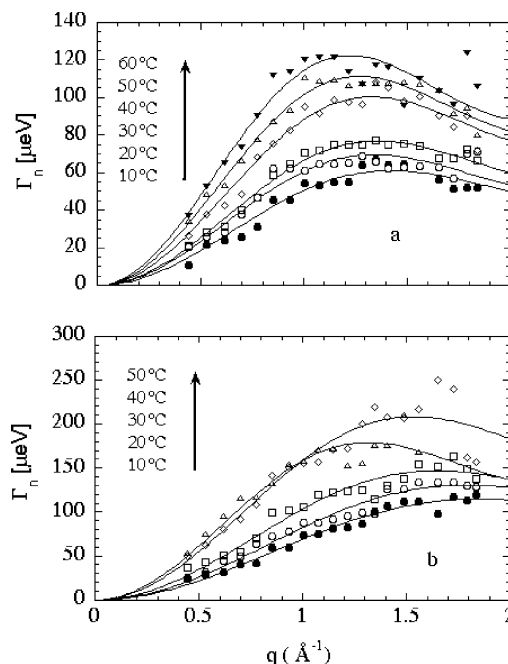


Figure 3. QENS line broadening of the Lorentzian describing the slow relaxing water molecules as a function of the scattering vector, q , at different temperatures. (a) PVAMA5 with a hydration degree of 60% (w/w) and (b) PVAMA5 at water saturation.

determination of structural and dynamic features of the microparticle hydrogels.

Analysis of the half-width at half-maximum, Γ_1 and Γ_2 , of the L_1 and L_2 Lorentzians provides an evaluation of the diffusion regime of the two sets of protons.

In cases (ii) and (iii), the scattering intensities, $I(q, \omega)$, have been described according to the following equation (eq 2):

$$S(q, \omega) = A\{p[\text{EISF}\delta(\omega) + (1 - \text{EISF})L_p] + (1 - p)[w_nL_n + (1 - w_n)L_b]\} + \text{bkg} \quad (2)$$

In this model, an explicit quasi-elastic term, $(1 - \text{EISF})L_p$, is introduced to account for the overall polymer moiety local motions. The distinction between slow relaxing and fast relaxing chains, as was done for the samples in D₂O, that is, case (i), is not allowed due to the major contribution provided by water. In eq 2, two quasi-elastic contributions, that is, $[w_nL_n + (1 - w_n)L_b]$, are included for slow and fast dynamics of water, respectively.

In the fitting procedure, the polymer and solvent mole fractions, p and $1 - p$, respectively, were fixed to the hydration degree determined experimentally. The other terms are the same as in eq 1. Moreover, in case (iii) the $(1 - w_n)L_b$ contribution also accounts for the possible presence of interstitial water around the PVAMA5 microparticles. However, this contribution, concerning the diffusion of unbound or loosely bound water, was not further analyzed due to its poorly defined origin and to the poor information content.

QENS experiments on PVAMA5 in H₂O focus on the solvent dynamics. In case (ii) and in case (iii), the line broadening of the Lorentzian contribution L_n , Γ_n , as a function of the scattering vector, q , displays a maximum at about 1.3 \AA^{-1} at all the investigated temperatures (Figure 3a,b).

This trend suggests for water molecules a stepwise diffusion with fixed length, that is, a Chudley–Elliot behavior,²² eq 3, at variance with the random jump diffusion, Singwi–Sjölander model,²³ eq 4, more often encountered in hydrogels.²⁴

$$\Gamma_n(q) = \frac{1}{\tau} \left[1 - \frac{\sin(ql)}{ql} \right] \quad (3)$$

$$\Gamma_n(q) = \frac{Dq^2}{1 + D\tau q^2} \quad (4)$$

Equations 3 and 4 relate the half-width at half-maximum, Γ_n , of the Lorentzian L_n with the water diffusion parameters τ , the average residence time in a diffusion site, l , the jump distance between sites, and D , the diffusion coefficient. The Chudley–Elliot model better describes the results obtained for (ii) and (iii) systems. Moreover, use of eq 4 as the fitting model yields unrealistic diffusion coefficient values, higher than those of bulk water. A similar Chudley–Elliot behavior was found by us on hydrated Sephadex samples.²⁵

The diffusion coefficients of bound water for the system PVAMA5 at water saturation and their dependence from the temperature were similar to those found for bulk water,²⁶ as shown in Figure 4. In system PVAMA5, with hydration degree of 60%, an average decrease of 25% in the diffusion coefficient values with respect to bulk water was determined (see Figure 4). Comparison with PVA hydrogels at water saturation, where the decrease of the diffusion coefficient was about 40%,¹¹ leads to the conclusion that the limited influence of PVAMA5 on the dynamic behavior of bound water can be attributed to the presence of polymethacrylate hydrophobic regions in the polymer network.

From the data of Figure 4, an activation energy of 4.3 ± 0.8 kcal/mol was determined for both systems (ii) and (iii), very close to the value measured in bulk water.^{26,27}

In case (i), that is, saturated D₂O, the weight of the quasi-elastic contribution of the more constrained polymeric moiety, $(1 - \text{EISF})p_1L_1$, compares to the contribution relative to the more flexible chains, $(1 - \text{EISF})(1 - p_1)L_2$, thereby describing the dynamics of the network regions more exposed to the solvent. The q -dependence of the broadening factor of the L_1 contribution, Γ_1 , discloses a confined dynamics of the polymer protons along a potential well of length equal to $L = 2\pi/q^*$,^{28,29} constant within the explored temperature range, as pointed out by the vertical arrow in Figure 5.

According to eq 5, $\Gamma_n(q \rightarrow 0)$ can be used to evaluate the diffusion coefficient, D , within a restricted volume or confined region²⁸

$$D = \frac{\Gamma_n(q \rightarrow 0)L^2}{\pi^2} \quad (5)$$

providing a value of 1×10^{-6} cm²/s. An increase of the diffusion coefficient observed above 50 °C can be an indication of an enhancement in the local mobility of the network chains.

The polymer matrix can influence the release process of the drug statically, acting as a sieve for the diffusing drug. This effect is minor when the release concerns a small molecule as DX compared to the polymer network meshes. However, the hydrogel matrix can influence the drug release if the localized diffusion of the chain segments occurs in a time scale comparable to that one relative to the drug release.

From the values of the diffusion coefficients obtained for the polymer segments of PVAMA5 between the cross-links of the matrix, a coupling can be expected with the release process of DX, typically characterized by similar diffusion coefficients. The case of PVAMA5 hydrogel represents a good example for illustrating the dynamic influence of the matrix on the drug release.

In view of a potential use of these microparticles as delivery device for anticancer drugs, we further developed the particles by increasing the particle charge by heterogeneous coupling of PVA microparticle hydrogels obtained from PVAMA5 (with a methacryloyl substitution equal to 5%), with succinic anhydride. Succinylation of PVAMA5 in solution followed by emulsion photoreticulation was soon abandoned due to the difficulty in achieving phase separation in water in the presence of charged PVA. However, succinylation was successfully achieved on the microparticles hydrogels PVAMA5. With this synthetic route, a degree of substitution of 3.6% of carboxylic groups with respect to PVAMA5 repeating units was obtained by potentiometric titration of the protonated particles. This product will be called hereafter PVAMA5S4. ζ -Potential measurements on succinoylated microparticles yielded a value of -21.5 mV to compare with the previously reported ζ -potential value of unsuccinoylated, that is, PVAMA5, of -14.5 mV.

Drug Loading and Release Features. The loading and release processes of DX were followed at 485 nm measuring the time dependence of the absorbance of the aqueous dispersion medium containing the drug, as described in the Experimental Section. Uptake of DX by dry PVAMA5S4 was carried out by a swelling equilibrium process in a DX aqueous solution at a concentration of 3.5×10^{-5} M. A payload capacity of 0.46 g of drug/g of PVAMA5S4 was determined for this system, corresponding to about 50% of the microparticles dry weight.

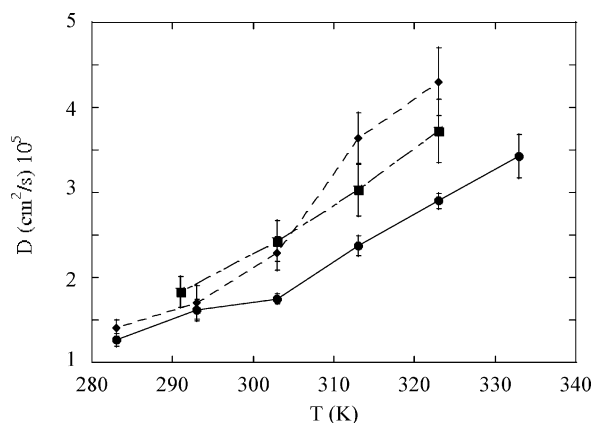


Figure 4. Temperature dependence of diffusion coefficients of bound water in systems: PVAMA5 at hydration degree 60% (●) and at water saturation (◆). Bulk water data from ref 26 (■).

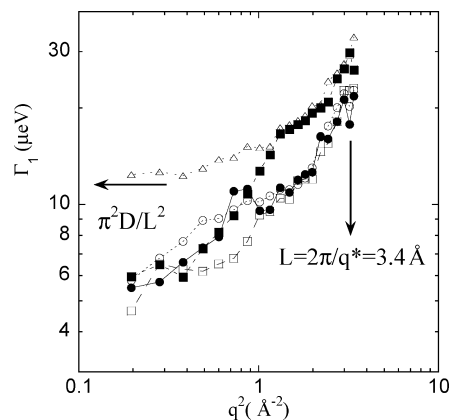


Figure 5. q^2 -Dependence of half-width at half-maximum of the QENS peak. Arrows indicate the low and high q regimes, respectively. ●, 10 °C; ○, 20 °C; □, 30 °C; ■, 50 °C; △, 60 °C.

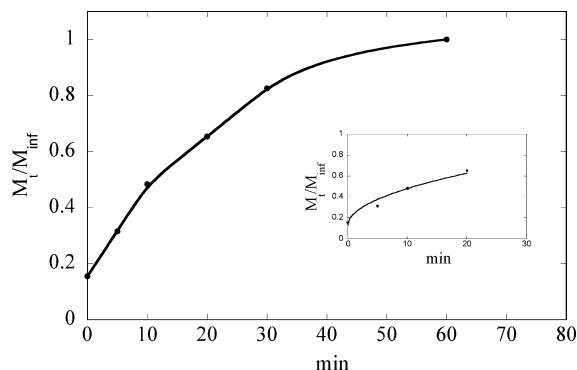


Figure 6. Cumulative amount of DX released from PVAMA5S4 microparticles as a function of time at room temperature. Insert: fitting of the initial release, according to a Fickian release of DX through the particles.

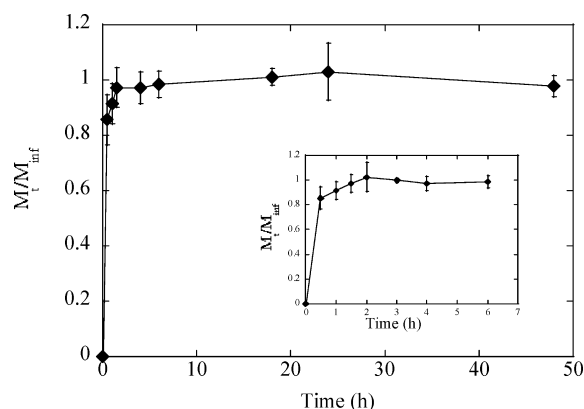


Figure 7. Cumulative amount of DX released from drug-loaded PVAMA5S4 microparticles (with a cargo amount of 1.5 mg doxorubicin per gram) in culture medium (pH 7.4) at 37 °C. Data represent mean values (\pm S.D.) of two independent experiments. Insert: early stage of the release up to 6 h.

This feature leaves a wide flexibility in tuning the amount of drug to be delivered.

In Figure 6, the release curve, described in terms of the cumulative molar index, M/M_{inf} , shows a burst with a complete drug release after about 1 h. The fit of the initial part of the curve, see insert of Figure 6, indicated that DX is released by microparticles according to Fickian diffusion-controlled process.

The kinetics of in vitro DX release from PVAMA5S4 microparticles with a cargo amount of 1.5 mg/g was studied in culture medium at 37 °C. As shown in Figure 7, release curve described in terms of the cumulative molar index, M/M_{inf} , shows an initial burst release (0.5 h) with a progressive increase in the extent of drug released within the first 2 h. Specifically, at this time point, the amount of DX measured in the medium corresponded to about 90% of the drug loaded onto microparticles. At later intervals, the amount of released DX remained almost constant. Comparison between the findings, shown in Figures 6 and 7 and obtained with different analytical approaches, indicates a similar DX release efficiency in water as well as in PBS buffer.

The cellular uptake of DX released from drug-loaded microparticles was then assayed in LoVo cells (Figure 8). A progressive enhancement in the cumulative amount of DX taken up by the cells was observed. Such an accumulation reached its maximum at 18 h and, at this time point, the quantity of DX internalized by cells represented about one tenth of the drug released in the culture medium from the drug-loaded microparticles.

A progressive reduction of the amount of internalized DX was observed at later time points, which could be partially

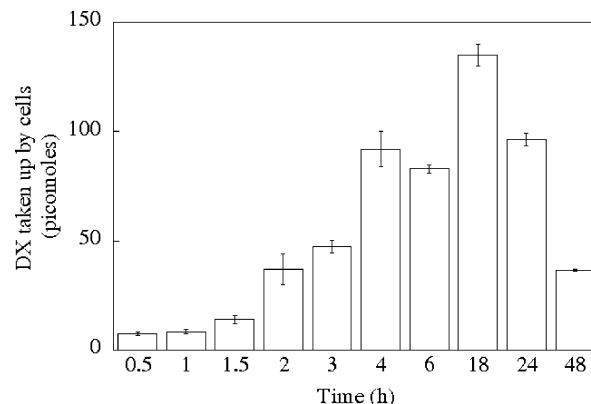


Figure 8. Uptake of DX released from drug-loaded PVAMA5S4 microparticles in LoVo cells. Data represent mean values (\pm S.D.) of two independent experiments.

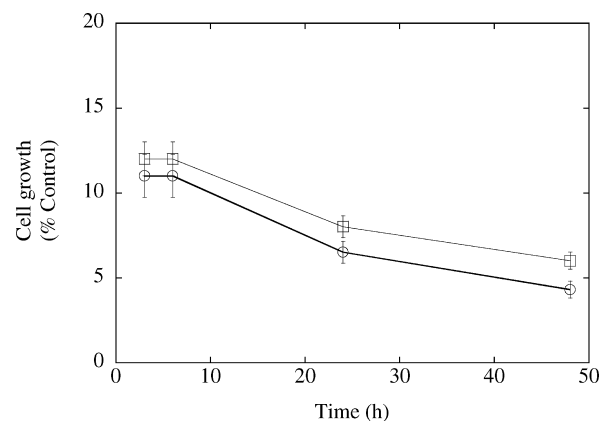


Figure 9. Antiproliferative activity of DX loaded onto microparticles (\square) and free DX (\circ) in LoVo cells, 72 h after drug exposure. Data are expressed as percentage of cell growth compared to controls and represent mean values (\pm S.D.) of two independent experiments.

explained by degradation of DX. In fact, it has been previously reported that the half-life of DX in an aqueous solution (pH 7.4) at 37 °C is approximately 48 h.³⁰ We then analyzed the cytotoxic effect of DX released from microparticles in LoVo cells (Figure 9).

Cells were incubated with drug-loaded microparticles for different intervals (ranging from 2 to 48 h) and the growth inhibitory activity exerted by the drug was assessed following an additional 72 h. A marked (>85%) reduction of cell number in drug-treated cultures compared to controls was consistently observed, starting from a drug exposure time of 2 h. For comparative purposes, we also assessed the effect of a 2–48 h exposure to 1.8 μ M (which corresponds to the highest concentration of DX in culture medium containing the drug-loaded microparticles) of free DX, and a growth inhibition curve similar to that obtained in LoVo cells exposed to DX released from the microparticles was observed (Figure 9).

Overall, these data confirm the possibility to use PVAMA5S4 microparticles for the delivery of DX and indicate that the drug loaded onto microparticles fully retains its anticancer activity.

Concluding Remarks

PVA-based microparticles can be considered a potential efficient way to deliver anticancer drugs by systemic administration. However, many aspects making such devices a real breakthrough in the drug delivery science, such as the enormous surface-to-volume ratio and the injectability in systemic circula-

tion, should be carefully understood in all their implications concerning cellular interactions. In this respect, response of the primary immune system and microparticles targeting are central issues to evaluate the efficacy of this new device. Probing the matrix for delivery at a molecular level, for example by neutrons, can provide information on the dynamics and on the hydration state of the particles. Incoherent QENS scattering can contribute also in understanding how the hydrogel structural features such as the cross-linking degree can influence the dynamics of the polymer chains and ultimately the delivery properties of the microparticles.

Different approaches are under way in the fast evolving panorama of the drug delivery science. Targeted particles derived from bacteria can undergo endocytosis and deliver a wide range of drugs by intracellular degradation.³¹ At present, it is difficult to forecast the future “ideal” platform for chemotherapy. However, modern drug delivery is providing a number of different approaches that will constitute the basis for the next generation of drug delivery devices.

Acknowledgment. This work was partially supported by INFM-FIRB Grant RBNE01XPYH. We thank Prof. A. Deriu and Dr. F. Sonvico of the University of Parma for ζ -potential measurements.

References and Notes

- (1) Amidon, G. L. *Mol. Pharmaceutics* **2004**, *1*, 1–1.
- (2) Spatz, J. *Soft Matter* **2007**, *3*, 261–262.
- (3) Langer, R.; Tirrell, D. A. *Nature* **2004**, *428*, 487–492.
- (4) Jackson, S. P.; Schoenwaelder, S. M. *Nat. Rev. Drug Discovery* **2003**, *2*, 775–789.
- (5) Lindman, S.; Lynch, I.; Thulin, E.; Nilsson, H.; Dawson, K. A.; Linse, S. *Nano Lett.* **2007**, *7*, 914–920.
- (6) <http://cordis.europa.eu/nanotechnology/nanomedicine.htm>.
- (7) Colvin, V. L. *Nat. Biotechnol.* **2003**, *21*, 1166–1170.
- (8) Linse, S.; Cabaleiro-Lago, C.; Xue, W.-F.; Lynch, I.; Lindman, S.; Thulin, E.; Radford, S. E.; Dawson, K. A. *Proc. Natl. Acad. Sci. U.S.A.* **2007**, *104*, 8691–8696.
- (9) Champion, J. A.; Mitragotri, S. *Proc. Natl. Acad. Sci. U.S.A.* **2006**, *103*, 4930–4934.
- (10) Cavalieri, F.; Miano, F.; D’Antona, P.; Paradossi, G. *Biomacromolecules* **2004**, *5*, 2439–2446.
- (11) Paradossi, G.; Cavalieri, F.; Chiessi, E.; Telling, M. T. F. *J. Phys. Chem. B* **2003**, *107*, 8363–8371.
- (12) Pridgen, E. M.; Langer, R.; Farokhzad, O. C. *Nanomed.* **2007**, *2*, 669–680.
- (13) van Dijk-Wolthuis, W. N. E.; Franssen, O.; Talsma, H.; van Steenberg, M. J.; Kettenes-van der Boch, J. J.; Hennink, W. E. *Macromolecules* **1995**, *28*, 6317–6322.
- (14) van Dijk-Wolthuis, W. N. E.; Kettenes-van der Boch, J. J.; van der Keek-van Hoof, A.; Hennink, W. E. *Macromolecules* **1997**, *30*, 3411–3413.
- (15) Franssen, O.; Hennink, W. E. *Int. J. Pharm.* **1998**, *168*, 1–7.
- (16) De Belder, A. N.; Granath, K. *Carbohydr. Res.* **1973**, *30*, 375–378.
- (17) Villa, R.; Zaffaroni, N.; Orlandi, L.; Bearzatto, A.; Costa, A.; Silvestrini, R. *Eur. J. Cancer* **1994**, *10*, 1534–1540.
- (18) Gianni, L.; Viganò, L.; Locatelli, A.; Capri, G.; Giani, A.; Tarenzi, E.; Bonadonna, G. *J. Clin. Oncol.* **1997**, *15*, 1906–1915.
- (19) Stenekes, R. J. H.; Hennink, W. E. *Int. J. Pharm.* **1999**, *189*, 131–135.
- (20) van Dijk-Wolthuis, W. N. E.; Hoogenboom, J. A. M.; van Steenberg, M. J.; Tsang, S. K. Y.; Hennink, W. E. *Macromolecules* **1997**, *30*, 4639–4645.
- (21) Bée, M. In *Quasielastic Neutron Scattering*; Hilger, A., Ed.; Elsevier Science: Bristol, 1988.
- (22) Chudley, G. T.; Elliott, R. J. *Proc. Phys. Soc.* **1961**, *77*, 353–361.
- (23) Singwi, K. S.; Sjölander, A. *Phys. Rev.* **1960**, *119*, 863–871.
- (24) Di Bari, M. T.; Deriu, A.; Albanese, G.; Cavatorta, F. *Chem. Phys.* **2003**, *292*, 333–339.
- (25) Cavalieri, F.; Chiessi, E.; Finelli, I.; Natali, F.; Paradossi, G.; Telling, M. F. *Macromol. Biosci.* **2006**, *6*, 579–589.
- (26) Krynicki, K.; Green, C. D.; Sawyer, D. W. *Faraday Discuss.* **1978**, *199*.
- (27) Texeira, J.; Bellisent-Funel, M. C.; Chen, S. H.; Dianoux, A. J. *Phys. Rev. A: At., Mol., Opt. Phys.* **1985**, *31*, 1913.
- (28) Volino, F.; Dianoux, A. J. *Mol. Phys.* **1980**, *41*, 271–279.
- (29) Hall, P. L.; Ross, D. K. *Mol. Phys.* **1981**, *42*, 673–682.
- (30) Beijinen, J. H.; van der Houwen, O. A.; G, J.; Underberg, W. J. M. *Int. J. Pharm.* **1986**, *32*, 123–131.
- (31) MacDiarmid, J. A.; Mugridge, N. B.; Weiss, J. C.; Phillips, L.; Burn, A. L.; et al. *Cancer Cell* **2007**, *11*, 431–445.

BM800225V